

OPTISHEAR: Towards Efficient and Adaptive Pruning of Large Language Models via Evolutionary Optimization

Shuqi Liu^{1,2}, Bowei He¹, Han Wu^{2,†}, Linqi Song^{1†}

¹ Department of Computer Science, City University of Hong Kong

² Huawei Noah’s Ark Lab

{shuqiliu4-c, boweihe2-c}@my.cityu.edu.hk

wu.han1@huawei.com

linqi.song@cityu.edu.hk

Abstract

Post-training pruning has emerged as a crucial optimization technique as large language models (LLMs) continue to grow rapidly. However, the significant variations in weight distributions across different LLMs make fixed pruning strategies inadequate for multiple models. In this paper, we introduce **OPTISHEAR**, an efficient evolutionary optimization framework for adaptive LLM pruning. Our framework features two key innovations: an effective search space built on our Meta pruning metric to handle diverse weight distributions, and a model-wise reconstruction error for rapid evaluation during search trials. We employ Non-dominated Sorting Genetic Algorithm III (NSGA-III) to optimize both pruning metrics and layerwise sparsity ratios. Through extensive evaluation on LLaMA-1/2/3 and Mistral models (7B-70B) across multiple benchmarks, we demonstrate that our adaptive pruning metrics consistently outperform existing methods. Additionally, our discovered layerwise sparsity ratios enhance the effectiveness of other pruning metrics. The framework exhibits strong cross-task and cross-model generalizability, providing a cost-effective solution for model compression.

1 Introduction

Large language models (LLMs) (Achiam et al., 2023; Touvron et al., 2023a; Le Scao et al., 2023) have demonstrated exceptional capabilities in language understanding and generation across various complex benchmarks (Bubeck et al., 2023; Wei et al., 2022a,b). However, their massive size poses significant challenges for inference and deployment due to extensive computational requirements. Model pruning has emerged as a promising compression technique, which reduces model size by setting specific weights to zero. While

traditional pruning approaches rely on retraining or iterative training to maintain performance (LeCun et al., 1989; Hassibi et al., 1993; Han et al., 2015; Liu et al., 2018; Blalock et al., 2020; Frankle and Carbin, 2018; Renda et al., 2019), these methods become impractical for billion-parameter LLMs. Consequently, post-training pruning (PTP) has gained increasing attention due to its resource efficiency. PTP methods work by developing metrics to assess weight importance, allowing for the removal of less critical weights without the need for retraining (Frantar and Alistarh, 2023; Sun et al., 2023; Zhang et al.).

However, as shown in Figure 1, we observe a significant performance drop when applying recent well-established pruning metrics (Frantar and Alistarh, 2023; Sun et al., 2023; Zhang et al.) to the LLaMA-3 (Meta, 2024) model. To analyze the reason for the performance drop, we demonstrate the distributions of input activation norms and weight magnitudes, two main components considered by recent pruning metrics. Despite the past success of SparseGPT (Frantar and Alistarh, 2023), Wanda (Sun et al., 2023), and RIA (Zhang et al.) on LLaMA-1 (Touvron et al., 2023a) and LLaMA-2 (Touvron et al., 2023b) models, the distinct weight distribution of LLaMA-3 underscores the limitations of using a fixed pruning metric across LLMs with varying weight distributions.

In this paper, we study the essential adaption of pruning strategy across different LLMs, and propose an efficient evolutionary optimization framework, named OPTISHEAR, to automatically search for the pruning strategy for different LLMs, including optimization of both the pruning metric and the layerwise sparsity ratios. In particular, we design an effective search space built on our Meta pruning metric. Unlike prior pruning metrics (Frantar and Alistarh, 2023; Sun et al., 2023; Zhang et al.) that consider weights and activations rely on fixed heuristics, our meta pruning metric dynamically

[†]Corresponding author.

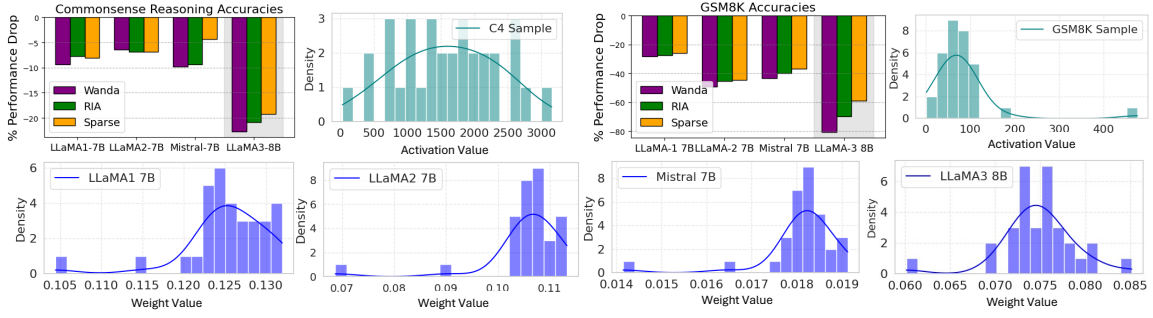


Figure 1: **Performance of existing pruning metrics on different LLMs.** Existing pruning metrics show significant performance drops on the LLaMA-3 model (bar charts in the upper part), influenced by its distinct weight distribution compared to LLaMA-1/2 and Mistral models (the lower part).

balances the relationship between weights and activations, to mitigate diverse weight distributions among different LLMs. Moreover, we also consider a better way for post-training pruning evaluations of each search trial. We show that prior evaluations based on perplexity (Dong et al., 2024) are more time-consuming and establish limited generalizability across different downstream tasks. Instead, we propose a lightweight search evaluation, model-wise reconstruction error, to speed up the evaluation. Finally, we apply NSGA-III (Deb and Jain, 2013; Jain and Deb, 2013) as our search algorithm, handling both the single-objective problem of pruning metric search and the multi-objective problem of layerwise sparsity ratio search in a unified framework.

We empirically evaluate OPTISHEAR on the widely adopted LLaMA-1, LLaMA-2, LLaMA-3 and Mistral models across multiple benchmarks. Our results demonstrate that, without any retraining or weight update, our OPTISHEAR-derived pruning metrics consistently outperform all established pruning metrics. Additionally, our OPTISHEAR-derived layerwise sparsity ratios could also boost the effectiveness of other pruning metrics that consider both weight and activation, such as Wanda and RIA. Furthermore, we verify the generalizability of our OPTISHEAR-derived pruning metrics through cross-task and cross-model evaluations, showing that metrics developed for complex arithmetic reasoning tasks also perform well on simpler tasks like language modeling, and remain effective when applied to models of different configurations.

2 Related Work

Emergent Large Features of LLMs Emergent large magnitude and massive activation features have been observed in Transformer-based large language models (Kovaleva et al., 2021; Puccetti et al.,

2022; Wei et al., 2022c; Dettmers et al., 2022; Sun et al., 2024). The occurrence of these hidden state features and input activations with large magnitudes is relatively rare, indicating the outlier patterns within model internal representations. However, these outlier features are shown to have essential importance in representing information, as zeroing out these outlier features during inference leads to a significant degradation in model performance (Dettmers et al., 2022; Sun et al., 2024). Recent development of quantization schemes (Lin et al., 2023; Dettmers et al., 2023; Xiao et al., 2023) and model pruning methods (Sun et al., 2023; Zhang et al.) for LLMs have been influenced by the presence of these outlier features. Our research expands on this insight by demonstrating that the relationship between these weights and input activation outlier features should also act as key indicators for selecting which weights to prune in LLMs.

Post-Training Pruning Post training pruning (PTP) has emerged as a popular technique for reducing the size and computational complexity of models without the need for extensive retraining (Hubara et al., 2021; Kwon et al., 2022; Frantar and Alistarh, 2023). Recent PTP methods for LLMs aim to evaluate the importance of weights using specific pruning metrics and remove less important weights by setting them to zero. Magnitude pruning (Han et al., 2015) directly removes weights based on their magnitude, offering simplicity but often resulting in unsatisfied performance for LLMs. To improve accuracy, SparseGPT (Frantar and Alistarh, 2023) solves layer-wise reconstruction problem, which significantly boosts performance but adds computational costs due to weight updates. Wanda (Sun et al., 2023) simplifies SparseGPT by considering only the product of weight magnitude and the norm of input activations. Building on Wanda, RIA (Zhang et al.) introduces a relative im-

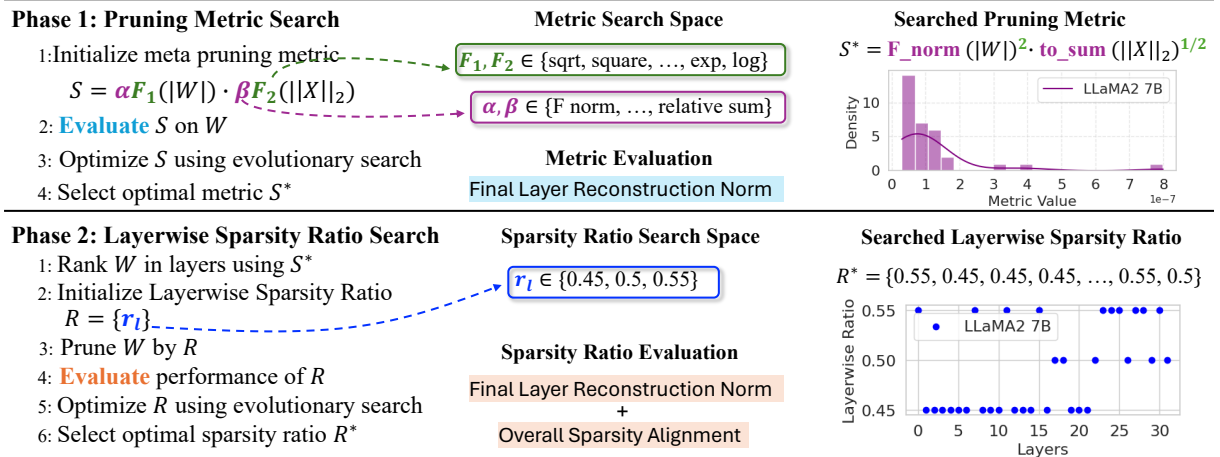


Figure 2: **Illustration of our proposed OPTISHEAR method.** OPTISHEAR consists of two phases: searching for the optimal pruning metric and the optimal layerwise sparsity ratios.

coefficient candidates for α, β	no coe, F norm, to sum, to mean, row sum, column sum, relative sum
operation candidates for F_1, F_2	no op, sqrt, square, sigmoid, softmax, exp, log

Table 1: Predefined coefficient and operation candidates for Meta Pruning Metric.

portance coefficient to enhance weight importance evaluation. These one-shot pruning metrics now stand out as strong baselines for LLM pruning.

3 OPTISHEAR

3.1 Method Overview

OPTISHEAR adapts pruning strategies to different LLMs through evolutionary optimization, automatically determining optimal pruning metrics and layer-specific sparsity ratios (Figure 2). During each search phase, OPTISHEAR samples pruning metrics or layerwise sparsity ratios from a predefined search space and evaluates their effectiveness. These evaluation results guide subsequent sampling decisions. 1) **Pruning Metric Search** - involves identifying the most effective metric for scoring the importance of model weights. 2) **Layerwise Sparsity Ratio Search** - determines the optimal proportion of weights to remove from each layer using the identified pruning metric.

3.2 Search Space

Meta Pruning Metric. Recent studies have revealed emergent properties in LLMs, including large weight magnitudes (Puccetti et al., 2022; Wei et al., 2022c; Dettmers et al., 2022) and massive input activations (Sun et al., 2024). Building on these findings, researchers (Sun et al., 2023; Zhang et al.) have improved pruning effectiveness by combining weight magnitudes with input activations.

We extend this approach by proposing a meta pruning metric that dynamically balances weights and activations based on each LLM’s weight distribution. Equation 1 defines our scoring mechanism for each weight W_{ij} using a weighted combination of weight magnitude and input activation:

$$S_{ij} = \alpha F_1(|W_{ij}|) \cdot \beta F_2(\|X_j\|_2). \quad (1)$$

The score combines weight magnitude $|W_{ij}|$ and input activation norm $\|X_j\|_2$ (calculated as the l_2 norm of feature j across tokens) through coefficients (α, β) and transformation functions (F_1, F_2). Table 1 lists the candidate coefficients and operations, with detailed calculations provided in Appendix A.6.

Our meta pruning metric generalizes existing approaches like Wanda and RIA. Wanda (Sun et al., 2023) uses a direct product of weight magnitude and input activation norm: $S_{ij} = |W_{ij}| \cdot \|X_j\|_2$, RIA (Zhang et al.) introduces relative importance (RI) for weights and applies a square root to the activation norm: $S_{ij} = \text{RI}(|W_{ij}|) \cdot \|X_j\|_2^{1/2}$. Our framework extends these metrics by allowing flexible coefficients and transformations for both terms, enabling more adaptive pruning strategies.

Layerwise Sparsity Ratios. Research has shown that neurons in different layers of Transformer architectures capture distinct types of information (Wang and Tu, 2020; Zhang et al., 2021). We leverage this insight by applying non-uniform pruning across layers: layers containing more critical

neurons receive lower pruning ratios, while those with less essential neurons undergo more aggressive pruning. We determine each layer’s sparsity ratio from three options: target sparsity - sparsity step, target sparsity, or target sparsity + sparsity step. The target sparsity represents the model’s overall pruning goal, while the sparsity step enables fine-tuned adjustments for layer-specific pruning. For LLMs with over 32 layers, our experiments show that using these three discrete sparsity options yields better results than larger sets when operating under limited search trials.

3.3 Search Evaluation.

The Search Evaluation phase guides the evolutionary process by assessing each candidate pruning strategy (Bäck and Schwefel, 1993). Aligned with the fundamental goal of model pruning—removing weights while maintaining performance (LeCun et al., 1989; Han et al., 2015)—OPTISHEAR employs two evaluation criteria: primary model-wise reconstruction error to assess pruning metric effectiveness, and secondary overall sparsity measurement to evaluate the layerwise sparsity ratios.

Model-wise Reconstruction Error. We introduce model-wise reconstruction error as a lightweight search evaluation metric for pruning strategies. While existing frameworks like PrunerZero (Dong et al., 2024) use perplexity for evaluation, our experiments show that perplexity-based evaluation is more time-consuming and exhibits poorer generalization across downstream tasks. Our proposed reconstruction error metric enables faster strategy evaluation while maintaining strong generalization capabilities. The model-wise reconstruction error f_{rec} quantifies the output discrepancy between the dense model θ and pruned model θ^* at the final layer. Given final layer input activations X_l , weight matrix $W_l \in \mathbb{R}^{r \times c}$ with r output and c input channels, and layer-specific sparsity masks M_i derived from importance scores, the reconstruction error is computed as:

$$f_{rec}(\theta, \theta^*) = \|W_l X_l - (M_l \odot W_l) \cdot X_l\|_{Frob}, \quad (2)$$

where $\|\cdot\|_{Frob}$ denotes the Frobenius norm (Golub and Van Loan, 1996), ensuring the pruned model’s outputs closely match the dense model’s outputs.

Sparsity Ratio Discrepancy. We introduce sparsity ratio discrepancy as a secondary evaluation measure since the layerwise sparsity search may result in overall model sparsity that deviates from the

pre-defined target. This occurs because the search assigns each layer a sampled sparsity ratio that can be slightly higher or lower than the pre-defined value. The sparsity ratio discrepancy f_{ratio} quantifies the difference between the achieved model sparsity and the pre-defined target ratio:

$$f_{ratio}(\theta, \theta^*) = \left| R_d - \frac{p(\theta) - p(\theta^*|\mathcal{R})}{p(\theta)} \right|. \quad (3)$$

where R_d is the pre-defined sparsity ratio, \mathcal{R} represents the layerwise sparsity ratios applied to the pruned model θ^* , and $p(\cdot)$ counts the total number of model parameters. The actual sparsity ratio is calculated as the fraction of removed parameters relative to the total parameters in the dense model.

3.4 Search Algorithm

We adopt the Non-dominated Sorting Genetic Algorithm III (NSGA-III) (Deb and Jain, 2013) as our search algorithm due to its ability to handle both single and multi-objective optimization problems, making it suitable for unified pruning metric and layerwise sparsity ratio searches. OPTISHEAR operates in two phases: first, it searches for optimal pruning metrics by minimizing the model-wise reconstruction error f_{rec} (Eq. 2). Second, it determines optimal layerwise sparsity ratios by jointly minimizing both f_{rec} and the sparsity ratio discrepancy f_{ratio} (Eq. 3). For the single-objective problem of pruning metric search, we aim to find:

$$s^* = \operatorname{argmin}_{s \in \mathcal{S}} f(s) \quad (4)$$

where s represents a candidate pruning strategy. For the multi-objective problem of layerwise sparsity ratio search, we define a vector of objective functions $\mathbf{F}(s) = (f_1(s), f_2(s), \dots, f_k(s))$. The goal is to find the Pareto optimal set:

$$\mathcal{S}^* = \{s \in \mathcal{S} \mid \nexists s' \in \mathcal{S} : \mathbf{F}(s') \prec \mathbf{F}(s)\} \quad (5)$$

where \prec denotes Pareto dominance.

4 Experiments

4.1 Setup

Models and Evaluations. We adopt four prominent open-sourcing LLMs as our foundation model, including LLaMA-1 (Touvron et al., 2023a) and LLaMA-2 (Touvron et al., 2023b) with sizes ranging from 7B to 70B, LLaMA-3 8B (Meta, 2024) and Mistral 7B (Jiang et al., 2023) with the base

Method	Weight Update	Sparsity	LLaMA-1		LLaMA-2		LLaMA-3		Mistral	
			7B	13B	7B	13B	8B	8B-Inst	7B	7B-Inst
LM Harness										
Dense	-	0%	59.70	62.58	59.72	63.03	64.21	64.15	60.06	66.69
Magnitude	✗	50%	46.89	47.34	52.40	52.90	44.87	45.31	57.24	63.34
SparseGPT	✓	50%	54.86	58.54	55.90	60.70	53.87	55.89	57.49	62.46
Wanda	✗	50%	54.08	59.18	55.89	60.88	49.66	51.34	54.20	61.04
RIA	✗	50%	55.10	59.45	55.67	61.03	50.76	50.64	54.39	60.48
Pruner-Zero	✗	50%	52.31	57.08	53.81	58.18	52.48	55.60	55.57	61.41
OPTISHEAR	✗	50%	55.10	59.73	57.47	61.42	55.50	55.94	59.33	63.51
WikiText Perplexity										
Dense	-	0%	5.37	4.80	5.04	4.56	5.80	7.91	5.23	4.90
Magnitude	✗	50%	13.27	13.55	11.96	6.16	73.93	5.5E2	7.14	6.59
SparseGPT	✓	50%	6.92	5.87	6.59	5.72	10.89	13.27	6.42	7.02
Wanda	✗	50%	6.90	5.82	6.47	5.64	10.57	16.37	7.24	7.22
RIA	✗	50%	6.81	5.83	6.43	5.63	12.56	15.57	7.27	7.21
Pruner-Zero	✗	50%	7.13	6.02	6.86	5.88	12.68	15.45	7.84	7.50
OPTISHEAR	✗	50%	6.78	5.74	6.35	5.51	9.23	11.37	6.22	6.55
GSM8K										
Dense	-	0%	11.07	17.82	14.59	19.86	52.39	74.45	40.11	47.76
Magnitude	✗	50%	1.52	5.99	2.05	6.22	1.97	1.29	15.53	27.37
SparseGPT	✓	50%	8.19	15.60	8.11	13.42	21.46	49.20	25.40	33.97
Wanda	✗	50%	7.96	11.52	7.43	9.10	10.16	32.68	22.74	33.59
RIA	✗	50%	8.04	11.14	7.96	9.25	15.85	52.39	24.18	32.15
Pruner-Zero	✗	50%	6.41	9.22	7.32	8.58	17.25	43.63	21.16	32.24
OPTISHEAR	✗	50%	8.14	15.37	8.13	13.79	41.17	52.39	25.31	35.25
w/ eval.	✗	50%	8.22	15.62	8.47	15.03	43.07	52.15	25.78	35.14
MMLU										
Dense	-	0%	35.28	46.98	41.97	51.47	65.23	66.35	58.92	62.54
Magnitude	✗	50%	26.24	30.12	26.04	43.83	4.36	12.03	50.83	49.52
SparseGPT	✓	50%	29.48	38.29	33.03	47.14	49.50	52.27	50.95	52.04
Wanda	✗	50%	29.81	37.84	32.09	48.06	49.05	53.15	53.05	53.62
RIA	✗	50%	30.37	37.79	31.46	47.39	48.99	54.02	52.67	53.14
Pruner-Zero	✗	50%	28.57	35.51	30.26	45.24	41.39	46.32	51.75	53.15
OPTISHEAR	✗	50%	30.93	38.80	32.24	48.15	50.65	55.11	53.10	53.77
w/ eval.	✗	50%	31.05	39.76	33.06	48.38	51.22	55.60	53.87	54.36

Table 2: Mean zero-shot accuracies(%) on the LM Harness, WikiText perplexity, GSM8K and MMLU accuracies(%) of pruned LLaMA-1/2/3 and Mistral models.

models and their instruction-tuned variants. Following previous works (Sun et al., 2023; Xia et al., 2023), we first evaluate on seven tasks from the EleutherAI LM Harness (Gao et al., 2023)¹, and the language modeling task based on the held-out WikiText (Merity et al., 2016) validation set. Furthermore, we also evaluate two more challenging tasks, arithmetic reasoning on GSM8K (Cobbe et al., 2021) and the language understanding benchmark MMLU (Hendrycks et al., 2020). For the comparison group settings, we follow Wanda (Sun et al., 2023) to compare and remove weights on a per-output basis, where weight importance scores are compared locally within each output neuron. We evaluate three sparsity types as defined in previous research (Sun et al., 2023; Zhang et al.): unstructured sparsity, semi-structured 4:8 and 2:4 sparsity.

¹Referred as *LM Harness* in remaining parts.

We conduct each search process with 350 trials. On a single NVIDIA RTX A6000 GPU, each trial takes less than 16 seconds for 8B models, making the search process computationally efficient. Detailed ablation studies on the number of trials and comprehensive search time analyses are provided in Appendix A.5 and Appendix A.4, respectively. **Baselines.** We compare OPTISHEAR with five existing baselines: Magnitude pruning (Han et al., 2015) which discards weights based on their magnitudes. SparseGPT (Frantar and Alistarh, 2023) solves the layer-wise reconstruction problem to identify redundant weights and prune them accordingly. Wanda (Sun et al., 2023) utilizes large-magnitude features and input activation to induce sparsity. RIA (Zhang et al.) further improves Wanda pruning by introducing the relative importance and channel permutation. Pruner-Zero (Dong et al., 2024) automatically searches for the opti-

Method	Weight Update	Sparsity	LLaMA-1		LLaMA-2		LLaMA-3		Mistral	
			7B	13B	7B	13B	8B	8B-Inst	7B	7B-Inst
WikiText Perplexity										
Magnitude	✗	4:8	17.48	16.80	16.10	7.23	2.5E2	5.6E2	8.78	8.67
SparseGPT	✓	4:8	8.16	7.05	7.89	6.54	15.57	16.62	7.71	8.15
Wanda	✗	4:8	8.19	6.95	8.01	6.60	16.82	21.52	8.95	8.42
RIA	✗	4:8	8.18	6.97	8.04	6.62	17.28	21.15	8.91	8.51
OPTISHEAR	✗	4:8	7.93	6.65	7.72	6.34	17.24	21.15	7.57	7.66
Magnitude	✗	2:4	49.06	19.33	38.50	9.04	5.3E3	5.3E3	13.18	11.83
SparseGPT	✓	2:4	10.58	8.53	10.38	8.26	23.43	26.68	10.17	9.84
Wanda	✗	2:4	11.04	9.06	11.31	8.46	31.89	59.12	13.54	11.08
RIA	✗	2:4	11.10	9.24	11.40	8.57	31.79	38.00	13.61	11.21
OPTISHEAR	✗	2:4	10.54	8.21	10.34	7.97	31.71	37.98	10.13	9.23
GSM8K										
Magnitude	✗	4:8	1.53	3.48	1.59	4.70	4.16	7.81	9.60	14.15
SparseGPT	✓	4:8	3.54	8.78	4.84	8.20	9.23	18.35	21.46	29.82
Wanda	✗	4:8	2.65	7.40	3.10	8.13	6.60	10.84	12.87	20.92
RIA	✗	4:8	3.17	8.74	2.93	7.75	8.12	17.59	17.36	27.18
OPTISHEAR	✗	4:8	3.71	9.29	4.95	8.53	8.38	17.59	21.80	30.39
Magnitude	✗	2:4	0.74	2.29	0.98	3.60	0.24	3.12	3.80	9.26
SparseGPT	✓	2:4	3.28	6.27	3.10	6.53	1.71	8.21	7.52	19.45
Wanda	✗	2:4	2.75	6.12	2.75	6.48	2.27	3.51	4.93	10.79
RIA	✗	2:4	2.56	4.73	2.79	5.65	1.98	6.74	6.49	17.22
OPTISHEAR	✗	2:4	3.34	6.27	3.41	6.72	2.52	6.74	7.91	20.33

Table 3: Evaluations of semi-structured N:M sparsity on WikiText and GSM8K datasets.

mal pruning metric based on weights and gradients, using perplexity as the evaluation measure.

Calibration Data. Calibration data is used to estimate input statistics from a small set of samples. For a fair comparison, we use the exact same calibration data as Wanda and SparseGPT when evaluating on LM Harness and WikiText, which includes 128 sequences sampled from the C4 training set (Raffel et al., 2020). For evaluations on GSM8K and MMLU, we randomly select 10 samples from the training dataset, each truncated to a sequence length of 512, as our calibration samples.

4.2 Main Results

LM Harness & Language Modeling. Table 2 shows our evaluation results on LM Harness and WikiText perplexity (detailed task-wise results in Appendix A.8). OPTISHEAR consistently outperforms all baseline methods across different models. Notably, while SparseGPT shows comparable performance to Wanda and RIA on LLaMA-1/2 models (Sun et al., 2023), it exhibits a significant performance gap on LLaMA-3 and Mistral models. Our OPTISHEAR framework achieves new state-of-the-art results across all model types, which we attribute to its adaptive pruning approach that accounts for different weight distributions between LLaMA-1/2 and LLaMA-3 models, as shown in Figure 1. Our evaluation extends to larger models

including LLaMA-30B and LLaMA2-70B, where OPTISHEAR maintains superior performance on both WikiText perplexity and LM Harness benchmarks. (in Appendix A.1 Table 8). Remarkably, when applied to LLaMA2-70B, OPTISHEAR achieves performance surpassing the dense model even without weight adjustment. We provide the **Arithmetic & Knowledge Reasoning**. For GSM8K and MMLU datasets in Table 2, OPTISHEAR consistently outperforms all baselines. The improvements are particularly pronounced on GSM8K, where OPTISHEAR achieves an accuracy of 41.17 on LLaMA-3 8B, nearly doubling the previous best result of 21.46. This substantial gap highlights the sensitivity of existing pruning methods to different model architectures. While OPTISHEAR is inherently task-agnostic, we found that incorporating validation set accuracy as an additional search objective further enhances performance beyond the standard OPTISHEAR approach. We provide detailed optimal metrics for each LLM in Appendix A.6.

Comparison to Pruner-Zero. As demonstrated in Table 2, OPTISHEAR significantly outperforms Pruner-Zero, while offering two key advantages: it achieves superior results without requiring computationally expensive gradient calculations, and it accelerates the pruning process 7-fold for LLaMA2-7B by employing model-wise reconstruction error

Method	Uniform	LLaMA-1		LLaMA-2		LLaMA-3		Mistral	
		7B	13B	7B	13B	8B	8B-Inst	7B	7B-Inst
Wanda	✓	6.90	5.82	6.47	5.64	10.57	16.37	7.24	7.22
Wanda w/ Ratio	✗	(+2.61)	(+3.09)	(+2.94)	(+2.13)	(+10.60)	(+16.49)	(+3.73)	(+3.32)
RIA	✓	6.81	5.83	6.43	5.63	12.56	15.57	7.27	7.21
RIA w/ Ratio	✗	(+2.35)	(+2.74)	(+2.64)	(+1.60)	(+12.58)	(+15.03)	(+5.23)	(+3.47)
OPTISHEAR wo/ Ratio	✓	6.75	5.75	6.32	5.52	9.23	11.37	6.22	6.55
OPTISHEAR	✗	(+2.07)	(+2.61)	(+2.06)	(+1.45)	(+3.03)	(+5.63)	(+2.25)	(+2.62)

Table 4: Our searched layerwise sparsity ratios are effective for both Wanda and RIA metrics. The number (%) in (·) denotes the relative improvement (RI). For instance, Wanda RI = (Wanda w/ Ratio - Wanda) / Wanda.

Method	WikiText				LM Harness			
	L1-7B	L2-7B	L3-8B	M-7B	L1-7B	L2-7B	L3-8B	M-7B
SparseGPT	6.92	6.59	10.89	6.42	54.86	55.90	53.87	57.49
OPTISHEAR	6.78	6.35	9.23	6.22	55.10	57.47	55.50	59.33
GSM8K Metric	6.78	6.39	12.78	6.23	55.15	56.05	55.59	57.66
Transferred Metric	6.76	6.35	9.23	6.16	55.24	57.47	55.50	58.30

Table 5: WikiText perplexity and zero-shot reasoning accuracy (%) with different pruning metrics.

instead of WikiText perplexity for evaluation.

N:M Semi-Structured Pruning. OPTISHEAR’s framework extends naturally to semi-structured N:M sparsity (Mishra et al., 2021), enabling hardware acceleration through NVIDIA’s sparse tensor cores. Table 3 shows that under 4:8 and 2:4 sparsity constraints, OPTISHEAR outperforms baselines on both WikiText and GSM8K datasets, with one notable exception: LLaMA-3 models. This exception likely stems from LLaMA-3’s higher knowledge density due to its larger training dataset (Meta, 2024), making it more sensitive to the continuous parameter blocks removed in semi-structured pruning—a limitation that requires SparseGPT’s weight updates for compensation.

4.3 Searched Layerwise Sparsity Ratios

Building on research showing varying parameter importance across layers (Wang and Tu, 2020; Zhang et al., 2021), OPTISHEAR implements layer-specific pruning ratios while maintaining 50% overall sparsity. Table 4 shows these optimized ratios enhance not only our model’s performance but also improve baseline methods like Wanda and RIA, achieving 4.68% better perplexity on WikiText and a 13.68% improvement for LLaMA-3 models. The detailed ratios in Appendix A.6 reveal higher redundancy in upper layers compared to lower layers, consistent with previous research findings.

4.4 Speedup

While SparseGPT has a computational complexity of $O(d_{hidden}^3)$, our meta pruning metric achieves a lower complexity of $O(d_{hidden}^2)$. Empirical measurements on NVIDIA RTX A6000 GPUs, us-

ing C4 dataset for calibration, confirm negligible pruning overhead when reducing models to 50% sparsity (Table 6). Furthermore, leveraging NVIDIA CUTLASS library’s GEMM kernel for semi-structured 4:8 and 2:4 sparsity implementations, we achieve an average 1.20× inference speedup compared to dense models (Table 7).

Method	L2-7B	L2-13B	L3-8B	M-7B
SparseGPT	370.03	464.77	457.71	450.76
OPTISHEAR	56.16	107.11	60.11	59.80

Table 6: Pruning speed for pruning LLaMA-2/3 and Mistral models to 50% sparsity.

Sparsity	L2-7B	L2-13B	L3-8B	M-7B
4:8	1.11×	1.04×	1.15×	1.17×
2:4	1.35×	1.14×	1.15×	1.16×

Table 7: Inference speedup of different sparsity patterns for LLaMA-2/3 and Mistral models.

5 In-depth Analysis

5.1 Pruning Metrics Generalizability

One potential limitation of OPTISHEAR is the computational cost of searching for optimal metrics and ratios across different models and datasets. We address this by investigating the transferability of our searched pruning metrics.

Cross-task Generalization. We investigate the transferability of pruning metrics from complex tasks (GSM8K arithmetic reasoning) to simpler ones (WikiText language modeling and LM Harness zero-shot reasoning), inspired by research showing complex demonstrations provide richer information (Fu et al., 2022). As shown in Table 5, metrics derived from GSM8K outperform

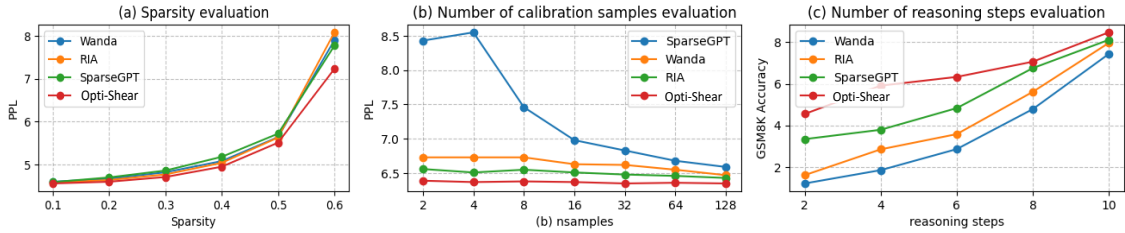


Figure 3: Sensitivity evaluation on sparsity, number of calibration samples (samples), and the reasoning steps in calibration samples for arithmetic reasoning.

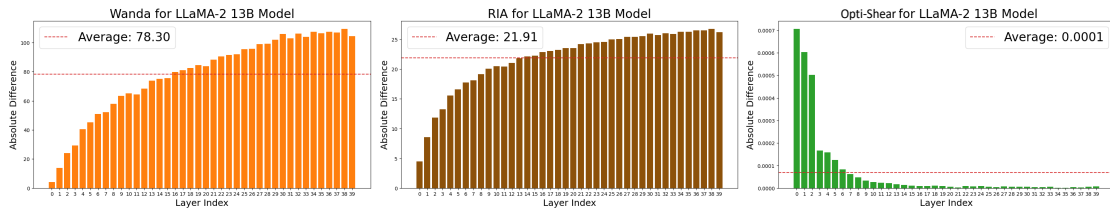


Figure 4: Layerwise absolute distance between transformed weights and transformed activations for Wanda, RIA, and OptiShear metrics on LLaMA-2 13B models.

SparseGPT and match task-specific metrics across LLaMA-1/2/3 and Mistral models on simpler tasks. **Cross-model Generalization.** We examine cross-model transferability using metrics derived from high-performing arithmetic reasoning models (LLaMA-2 7B and LLaMA-3 8B). The LLaMA-3 metric is applied to Mistral models, while the LLaMA-2 metric is tested on LLaMA-1 models. Attempts to transfer LLaMA-3 metrics to LLaMA-1/2 models proved ineffective, likely due to substantial differences in weight distributions. Table 5 shows metrics from superior models not only outperform baselines but also surpass the original OPTISHEAR. Therefore, although we still claim the necessity of adaptive pruning for different models, we also provide a cost-effective alternative to mitigate the search process, which is adopting the pruning metric identified on the challenging task with the strongest model in your candidate pool. This metric has demonstrated a capacity for generalization, proving transferrable and reusable across less complex tasks or the less-performing models.

5.2 Sparsity & Calibration Samples

In Figure 3(a), we evaluate LLaMA-2 13B under different sparsity ratios (0.1-0.6). OPTISHEAR consistently outperforms all baselines, achieving a 10.52% relative improvement over RIA at 60Figure 3(b) examines calibration sample size impact (2-128) on LLaMA2-7B. While SparseGPT’s performance varies with sample size, OPTISHEAR maintains superior results even with limited samples.

For arithmetic reasoning (Figure 3(c)), increasing reasoning steps in calibration samples improves accuracy across all methods, with OPTISHEAR showing consistent advantages. Further analyses of search algorithms, robustness, and search space are provided in Appendices A.2 and A.3.

5.3 Insights from Optimal Pruning Metrics

Our analysis reveals that the effectiveness of pruning metrics is influenced by the gap between transformed weights and activations. Figure 4 demonstrates that while RIA reduces this gap compared to Wanda, OPTISHEAR’s searched metric nearly eliminates it through weighted transformation that normalizes both components into a comparable range. The superior performance shown in Table 2 suggests that minimizing this transformation gap leads to more effective pruning. Detailed analysis on other LLMs is provided in Appendix A.7.

6 Conclusion

In this work, we propose an adaptive pruning strategy search framework, named OPTISHEAR, to automatically identify the optimal pruning metrics and layerwise pruning ratios for LLMs with varying weight distributions. Inspired by the discovery of significant weight and activation features in LLMs, we create a meta pruning metric to balance these magnitudes. OPTISHEAR identifies effective sparse networks in pretrained LLMs without re-training. Our evaluation shows that the metric from the best model for arithmetic reasoning also excels in simpler tasks with similar weight distributions.

Limitations

While OptiShear demonstrates promising results in adaptive pruning for large language models, there are several limitations to consider. For example, OptiShear shows reduced effectiveness on LLaMA-3 models under semi-structured pruning constraints (4:8 and 2:4 sparsity patterns). This limitation likely stems from two factors: (1) the model’s higher knowledge density making it more sensitive to parameter block removal, and (2) the more complex weight distribution patterns in newer architectures that challenge our current search space design. Performance degradation becomes particularly noticeable at sparsity rates above 50% under these structured constraints. Additionally, while OptiShear’s pruning metrics successfully generalize from complex to simpler tasks within the same model family, they demonstrate limited transferability across architectures with fundamentally different weight distributions. For example, metrics optimized for LLaMA-3 show poor performance when applied to LLaMA-1/2 models, suggesting that the underlying weight transformation mechanisms may be too model-specific. This limitation necessitates separate optimization processes for different model families, increasing the overall computational cost for organizations maintaining multiple model types.

Future research directions could address these limitations through more efficient search algorithms, architecture-agnostic pruning strategies, and improved transferability across model families. Additionally, investigating hybrid approaches that combine the benefits of different pruning paradigms might help mitigate some of these constraints.

Ethics Statement

This study utilizes publicly available datasets for our models. Prior research endeavors have generally taken ethical considerations into account. We have manually inspected a subset of samples and found no explicit ethical concerns, including violent or offensive content. Nonetheless, it is crucial to highlight that the output generated by large language models lacks the degree of control we might assume. Consequently, we are prepared to implement measures to mitigate any unforeseen outputs.

References

- Josh Achiam, Steven Adler, Sandhini Agarwal, Lama Ahmad, Ilge Akkaya, Florencia Leoni Aleman, Diogo Almeida, Janko Altschmidt, Sam Altman, Shyamal Anadkat, et al. 2023. Gpt-4 technical report. *arXiv preprint arXiv:2303.08774*.
- Thomas Bäck and Hans-Paul Schwefel. 1993. An overview of evolutionary algorithms for parameter optimization. *Evolutionary computation*, 1(1):1–23.
- James Bergstra, Rémi Bardenet, Yoshua Bengio, and Balázs Kégl. 2011. Algorithms for hyper-parameter optimization. *Advances in neural information processing systems*, 24.
- James Bergstra and Yoshua Bengio. 2012. Random search for hyper-parameter optimization. *Journal of machine learning research*, 13(2).
- James Bergstra, Daniel Yamins, and David Cox. 2013. Making a science of model search: Hyperparameter optimization in hundreds of dimensions for vision architectures. In *International conference on machine learning*, pages 115–123. PMLR.
- Davis Blalock, Jose Javier Gonzalez Ortiz, Jonathan Frankle, and John Gutttag. 2020. What is the state of neural network pruning? *Proceedings of machine learning and systems*, 2:129–146.
- Sébastien Bubeck, Varun Chandrasekaran, Ronen Eldan, Johannes Gehrke, Eric Horvitz, Ece Kamar, Peter Lee, Yin Tat Lee, Yuanzhi Li, Scott Lundberg, et al. 2023. Sparks of artificial general intelligence: Early experiments with gpt-4. *arXiv preprint arXiv:2303.12712*.
- Christopher Clark, Kenton Lee, Ming-Wei Chang, Tom Kwiatkowski, Michael Collins, and Kristina Toutanova. 2019. Boolq: Exploring the surprising difficulty of natural yes/no questions. In *Proceedings of the 2019 Conference of the North American Chapter of the Association for Computational Linguistics: Human Language Technologies, Volume 1 (Long and Short Papers)*, pages 2924–2936.
- Peter Clark, Isaac Cowhey, Oren Etzioni, Tushar Khot, Ashish Sabharwal, Carissa Schoenick, and Oyvind Tafjord. 2018. Think you have solved question answering? try arc, the ai2 reasoning challenge. *arXiv preprint arXiv:1803.05457*.
- Karl Cobbe, Vineet Kosaraju, Mohammad Bavarian, Mark Chen, Heewoo Jun, Lukasz Kaiser, Matthias Plappert, Jerry Tworek, Jacob Hilton, Reiichiro Nakano, et al. 2021. Training verifiers to solve math word problems. *arXiv preprint arXiv:2110.14168*.
- Kalyanmoy Deb and Himanshu Jain. 2013. An evolutionary many-objective optimization algorithm using reference-point-based nondominated sorting approach, part i: solving problems with box constraints. *IEEE transactions on evolutionary computation*, 18(4):577–601.

- Kalyanmoy Deb, Amrit Pratap, Sameer Agarwal, and TAMT Meyarivan. 2002. A fast and elitist multiobjective genetic algorithm: Nsga-ii. *IEEE transactions on evolutionary computation*, 6(2):182–197.
- Tim Dettmers, Mike Lewis, Younes Belkada, and Luke Zettlemoyer. 2022. Gpt3. int8 (): 8-bit matrix multiplication for transformers at scale. *Advances in Neural Information Processing Systems*, 35:30318–30332.
- Tim Dettmers, Ruslan Svirschevski, Vage Egiazarian, Denis Kuznedelev, Elias Frantar, Saleh Ashkboos, Alexander Borzunov, Torsten Hoeffler, and Dan Alistarh. 2023. Spqr: A sparse-quantized representation for near-lossless llm weight compression. *arXiv preprint arXiv:2306.03078*.
- Peijie Dong, Lujun Li, Zhenheng Tang, Xiang Liu, Xinglin Pan, Qiang Wang, and Xiaowen Chu. 2024. Pruner-zero: Evolving symbolic pruning metric from scratch for large language models. In *Forty-first International Conference on Machine Learning*.
- Jonathan Frankle and Michael Carbin. 2018. The lottery ticket hypothesis: Finding sparse, trainable neural networks. In *International Conference on Learning Representations*.
- Elias Frantar and Dan Alistarh. 2023. Sparsegpt: Massive language models can be accurately pruned in one-shot. In *International Conference on Machine Learning*, pages 10323–10337. PMLR.
- Yao Fu, Hao Peng, Ashish Sabharwal, Peter Clark, and Tushar Khot. 2022. Complexity-based prompting for multi-step reasoning. In *The Eleventh International Conference on Learning Representations*.
- Leo Gao, Jonathan Tow, Baber Abbasi, Stella Biderman, Sid Black, Anthony DiPofi, Charles Foster, Laurence Golding, Jeffrey Hsu, Alain Le Noac’h, Haonan Li, Kyle McDonell, Niklas Muennighoff, Chris Ociepa, Jason Phang, Laria Reynolds, Hailey Schoelkopf, Aviya Skowron, Lintang Sutawika, Eric Tang, Anish Thite, Ben Wang, Kevin Wang, and Andy Zou. 2023. [A framework for few-shot language model evaluation](#).
- Gene H Golub and Charles F Van Loan. 1996. Matrix computations.
- Song Han, Jeff Pool, John Tran, and William Dally. 2015. Learning both weights and connections for efficient neural network. *Advances in neural information processing systems*, 28.
- Babak Hassibi, David G Stork, and Gregory J Wolff. 1993. Optimal brain surgeon and general network pruning. In *IEEE international conference on neural networks*, pages 293–299. IEEE.
- Dan Hendrycks, Collin Burns, Steven Basart, Andy Zou, Mantas Mazeika, Dawn Song, and Jacob Steinhardt. 2020. Measuring massive multitask language understanding. In *International Conference on Learning Representations*.
- Itay Hubara, Brian Chmiel, Moshe Isard, Ron Banner, Joseph Naor, and Daniel Soudry. 2021. Accelerated sparse neural training: A provable and efficient method to find n: m transposable masks. *Advances in neural information processing systems*, 34:21099–21111.
- Himanshu Jain and Kalyanmoy Deb. 2013. An evolutionary many-objective optimization algorithm using reference-point based nondominated sorting approach, part ii: Handling constraints and extending to an adaptive approach. *IEEE Transactions on evolutionary computation*, 18(4):602–622.
- Albert Q Jiang, Alexandre Sablayrolles, Arthur Mensch, Chris Bamford, Devendra Singh Chaplot, Diego de las Casas, Florian Bressand, Gianna Lengyel, Guillaume Lample, Lucile Saulnier, et al. 2023. Mistral 7b. *arXiv preprint arXiv:2310.06825*.
- Olga Kovaleva, Saurabh Kulshreshtha, Anna Rogers, and Anna Rumshisky. 2021. Bert busters: Outlier dimensions that disrupt transformers. *Findings of the Association for Computational Linguistics: ACL-IJCNLP 2021*.
- Woosuk Kwon, Sehoon Kim, Michael W Mahoney, Joseph Hassoun, Kurt Keutzer, and Amir Gholami. 2022. A fast post-training pruning framework for transformers. *Advances in Neural Information Processing Systems*, 35:24101–24116.
- Teven Le Scao, Angela Fan, Christopher Akiki, Elie Pavlick, Suzana Ilić, Daniel Hesslow, Roman Castagné, Alexandra Sasha Luccioni, François Yvon, Matthias Gallé, et al. 2023. Bloom: A 176b-parameter open-access multilingual language model.
- Yann LeCun, John Denker, and Sara Solla. 1989. Optimal brain damage. *Advances in neural information processing systems*, 2.
- Ji Lin, Jiaming Tang, Haotian Tang, Shang Yang, Xingyu Dang, and Song Han. 2023. Awq: Activation-aware weight quantization for llm compression and acceleration. *arXiv preprint arXiv:2306.00978*.
- Zhuang Liu, Mingjie Sun, Tinghui Zhou, Gao Huang, and Trevor Darrell. 2018. Rethinking the value of network pruning. In *International Conference on Learning Representations*.
- Stephen Merity, Caiming Xiong, James Bradbury, and Richard Socher. 2016. Pointer sentinel mixture models. *arXiv preprint arXiv:1609.07843*.
- Meta. 2024. [Introducing meta llama 3: The most capable openly available llm to date](#).
- Todor Mihaylov, Peter Clark, Tushar Khot, and Ashish Sabharwal. 2018. Can a suit of armor conduct electricity? a new dataset for open book question answering. *arXiv preprint arXiv:1809.02789*.

- Asit Mishra, Jorge Albericio Latorre, Jeff Pool, Darko Stosic, Dusan Stosic, Ganesh Venkatesh, Chong Yu, and Paulius Micikevicius. 2021. Accelerating sparse deep neural networks. *arXiv preprint arXiv:2104.08378*.
- Yoshihiko Ozaki, Yuki Tanigaki, Shuhei Watanabe, Masahiro Nomura, and Masaki Onishi. 2022. Multiobjective tree-structured parzen estimator. *Journal of Artificial Intelligence Research*, 73:1209–1250.
- Giovanni Puccetti, Anna Rogers, Aleksandr Drozd, and Felice Dell’Orletta. 2022. Outliers dimensions that disrupt transformers are driven by frequency. *arXiv preprint arXiv:2205.11380*.
- Colin Raffel, Noam Shazeer, Adam Roberts, Katherine Lee, Sharan Narang, Michael Matena, Yanqi Zhou, Wei Li, and Peter J Liu. 2020. Exploring the limits of transfer learning with a unified text-to-text transformer. *Journal of machine learning research*, 21(140):1–67.
- Alex Renda, Jonathan Frankle, and Michael Carbin. 2019. Comparing rewinding and fine-tuning in neural network pruning. In *International Conference on Learning Representations*.
- Keisuke Sakaguchi, Ronan Le Bras, Chandra Bhagavatula, and Yejin Choi. 2021. Winogrande: An adversarial winograd schema challenge at scale. *Communications of the ACM*, 64(9):99–106.
- Mingjie Sun, Xinlei Chen, J Zico Kolter, and Zhuang Liu. 2024. Massive activations in large language models. *arXiv preprint arXiv:2402.17762*.
- Mingjie Sun, Zhuang Liu, Anna Bair, and J Zico Kolter. 2023. A simple and effective pruning approach for large language models. In *The Twelfth International Conference on Learning Representations*.
- Hugo Touvron, Thibaut Lavril, Gautier Izacard, Xavier Martinet, Marie-Anne Lachaux, Timothée Lacroix, Baptiste Rozière, Naman Goyal, Eric Hambro, Faisal Azhar, et al. 2023a. Llama: Open and efficient foundation language models. *arXiv preprint arXiv:2302.13971*.
- Hugo Touvron, Louis Martin, Kevin Stone, Peter Albert, Amjad Almahairi, Yasmine Babaei, Nikolay Bashlykov, Soumya Batra, Prajjwal Bhargava, Shrutu Bhosale, et al. 2023b. Llama 2: Open foundation and fine-tuned chat models. *arXiv preprint arXiv:2307.09288*.
- Alex Wang, Amanpreet Singh, Julian Michael, Felix Hill, Omer Levy, and Samuel Bowman. 2018. Glue: A multi-task benchmark and analysis platform for natural language understanding. In *Proceedings of the 2018 EMNLP Workshop BlackboxNLP: Analyzing and Interpreting Neural Networks for NLP*, pages 353–355.
- Wenxuan Wang and Zhaopeng Tu. 2020. Rethinking the value of transformer components. In *Proceedings of the 28th International Conference on Computational Linguistics*, pages 6019–6029.
- Jason Wei, Yi Tay, Rishi Bommasani, Colin Raffel, Barret Zoph, Sebastian Borgeaud, Dani Yogatama, Maarten Bosma, Denny Zhou, Donald Metzler, et al. 2022a. Emergent abilities of large language models. *arXiv preprint arXiv:2206.07682*.
- Jason Wei, Xuezhi Wang, Dale Schuurmans, Maarten Bosma, Fei Xia, Ed Chi, Quoc V Le, Denny Zhou, et al. 2022b. Chain-of-thought prompting elicits reasoning in large language models. *Advances in neural information processing systems*, 35:24824–24837.
- Xiuying Wei, Yunchen Zhang, Xiangguo Zhang, Ruihao Gong, Shanghang Zhang, Qi Zhang, Fengwei Yu, and Xianglong Liu. 2022c. Outlier suppression: Pushing the limit of low-bit transformer language models. *Advances in Neural Information Processing Systems*, 35:17402–17414.
- Mengzhou Xia, Tianyu Gao, Zhiyuan Zeng, and Danqi Chen. 2023. Sheared llama: Accelerating language model pre-training via structured pruning. In *The Twelfth International Conference on Learning Representations*.
- Guangxuan Xiao, Ji Lin, Mickael Seznec, Hao Wu, Julien Demouth, and Song Han. 2023. Smoothquant: Accurate and efficient post-training quantization for large language models. In *International Conference on Machine Learning*, pages 38087–38099. PMLR.
- Rowan Zellers, Ari Holtzman, Yonatan Bisk, Ali Farhadi, and Yejin Choi. 2019. Hellaswag: Can a machine really finish your sentence? In *Proceedings of the 57th Annual Meeting of the Association for Computational Linguistics*. Association for Computational Linguistics.
- Yingtao Zhang, Haoli Bai, Haokun Lin, Jialin Zhao, Lu Hou, and Carlo Vittorio Cannistraci. Plug-and-play: An efficient post-training pruning method for large language models. In *The Twelfth International Conference on Learning Representations*.
- Zhengyan Zhang, Yankai Lin, Zhiyuan Liu, Peng Li, Maosong Sun, and Jie Zhou. 2021. Moefication: Transformer feed-forward layers are mixtures of experts. *arXiv preprint arXiv:2110.01786*.

Model	Method	WikiText	BoolQ	RTE	HellaSwag	WinoGrande	ARC-e	ARC-c	OBQA	Average
LLaMA 30B	Dense	4.77	82.69	66.79	63.35	75.69	80.30	52.82	36.00	65.38
	Magnitude	7.55	64.34	50.18	50.59	66.54	72.39	43.77	29.00	53.83
	SparseGPT	5.32	82.32	62.45	59.15	75.22	78.96	48.56	35.00	63.09
	Wanda	5.98	81.90	65.34	60.93	73.48	79.29	49.66	34.60	63.60
	RIA	5.16	83.36	67.15	60.01	72.85	78.70	48.29	33.60	63.42
	OPTISHEAR	5.10	83.36	67.51	60.93	72.61	78.91	49.74	34.20	63.89
LLaMA2 70B	Dense	3.12	83.40	67.87	66.10	78.06	82.55	54.44	37.20	67.08
	Magnitude	4.98	70.55	60.65	61.50	73.48	75.70	49.23	35.40	60.93
	SparseGPT	3.98	83.55	70.40	63.80	78.85	82.40	53.75	38.20	67.28
	Wanda	3.99	82.50	73.65	64.10	78.14	80.80	52.65	37.40	67.03
	RIA	3.91	83.25	71.49	64.05	77.74	81.20	53.16	36.60	66.77
	OPTISHEAR	3.86	83.25	73.21	64.00	78.48	81.25	53.07	38.40	67.38

Table 8: WikiText perplexity and mean zero-shot accuracies(%) on the LM Harness of 50% unstructured pruned LLaMA-1 30B and LLaMA-2 70B models.

A Appendix

A.1 Effectiveness on Super Large Language Models

We also explore the effectiveness of OPTISHEAR when scaling up the model size. As shown in Table 8, OPTISHEAR consistently outperforms the existing methods across the board.

A.2 Ablation Study on Search Algorithms and Robustness Analysis

We conduct a robustness analysis using five search algorithms, including random search (Bergstra and Bengio, 2012), which randomly samples hyperparameter values from a predefined search space and does not take into account any information about the performance of previous trials, the Tree-structured Parzen Estimator (TPE) (Bergstra et al., 2011, 2013; Ozaki et al., 2022), a Bayesian optimization algorithm that uses a tree structure to model the relationship between hyperparameters and the objective function, and Quasi-Monte Carlo (QMC) (Bergstra and Bengio, 2012) sampler, which generates a sequence of points that cover the search space more evenly compared to random sampling, for more efficient exploration. Additionally, we utilize the state-of-the-art multi-objective optimization algorithms Non-dominated Sorting Genetic Algorithm II (NSGA-II) (Deb et al., 2002) and NSGA-III (Deb and Jain, 2013; Jain and Deb, 2013), which are based on genetic algorithms and optimize multiple conflicting objectives simultaneously. NSGA-II uses a non-dominated sorting approach to rank solutions based on their dominance relationship, while NSGA-III extends NSGA-II by incorporating reference points to guide the search toward the Pareto front.

Table 9 presents the statistical analysis, specifically the mean and standard deviation, of the per-

formance of pruned LLaMA-2 7B models across four distinct benchmarks. To validate the robustness and reliability of our results, each model was evaluated using three different search processes, each initialized with different random seeds. We report the performance outcomes of the NSGA-III search method in the main paper, as it generally outperforms other algorithms.

A.3 Ablation Study on Search Space

In Table 10, we construct the sub-search spaces by randomly selecting 2-6 coefficients/operations from our candidate pool. We test three different subspaces using random seeds 0, 42, and 100. The evaluations are conducted on WikiText, and the perplexity scores are reported below. We can see that the search performed on the full set consistently yields the best results. An interesting observation is that using a very small subspace may lead to extremely poor outcomes. This occurs because the candidate coefficients/operations in the subspace are all unsuitable for the target model.

A.4 Search Cost

In Table 11, we provide the detailed search time consumed on a single Nvidia RTX A6000 GPU. We report the total time of 350 search trials, as we empirically found that the optimal value is generally obtained within these rounds, as illustrated in Figure 4(c). As shown in the table, the time of an optimal search is within 2.5 GPU hours. With multiple GPUs, the search process can generally be finished within 1 hour. Therefore, we believe that the search cost of our method is moderate and acceptable.

A.5 Hyperparameter Analysis

We evaluate the impact of various hyperparameters applied in the layerwise sparsity ratios search

Dataset	Random	TPE	QMC	NSGA-II	NSGA-III
WikiText	6.89 (± 0.0671)	6.33 (± 0.0714)	6.39 (± 0.0700)	6.44 (± 0.0632)	6.35 (± 0.0640)
GSM8K	7.96 (± 0.2406)	8.33 (± 0.2498)	8.08 (± 0.2220)	8.47 (± 0.2479)	8.49 (± 0.2646)
MMLU	31.11 (± 0.3962)	31.06 (± 0.4017)	31.80 (± 0.4400)	32.43 (± 0.4701)	33.06 (± 0.4687)
LM-harness	55.32 (± 0.5300)	55.74 (± 0.5367)	56.19 (± 0.5234)	56.59 (± 0.5689)	57.47 (± 0.5718)

Table 9: Statistical results of different search algorithms on LLaMA-2 7B model. We report the mean and standard deviation under 3 search process runs.

Seed	2 Ops & 2 Coes	3 Ops & 3 Coes	4 Ops & 4 Coes	5 Ops & 5 Coes	6 Ops & 6 Coes	Full Search Space
0	870.16	753.32	6.43	6.51	6.57	6.35
42	6.47	6.39	6.39	6.39	6.35	6.35
100	6.43	6.43	6.43	6.58	6.58	6.35

Table 10: WikiText perplexity for random subspaces of the search space on LLaMA2-7B model in searching for optimal pruning metric.

procession the performance of WikiText perplexity. We use the LLaMA-2 7B model and prune to unstructured 50% sparsity.

Sparsity step. In layerwise sparsity ratio search, we identify the optimal sparsity ratio for each layer by selecting from a predefined sparsity ratio set: [target sparsity - sparsity step, target sparsity, target sparsity + sparsity step]. Here, target sparsity is the pre-defined sparsity ratio for pruning the overall model. The sparsity step allows for adjustments to achieve slightly higher or lower sparsity ratios.

In Figure 5(a), we vary the sparsity step ranging between 3% and 10%. We empirically find that a 5% sparsity step usually performs better than other sparsity steps, such as lower 3% or higher 8% and 10%. This is possibly because smaller steps might

not significantly reduce redundancy, while larger steps might overly simplify the layers, leading to a loss of important features and a decrease on overall model performance.

Number of sparsity ratios. In Figure 5(b), we fix the sparsity step as 5% and vary the number of sparsity ratios in the predefined sparsity ratio set, which ranges from 3 to 9. Specifically, one sparsity ratio in the sparsity ratio set corresponds to uniform pruning across layers. For example, a predefined sparsity ratio set with 5 sparsity ratios is defined as [target sparsity - 2*sparsity step, target sparsity - sparsity step, target sparsity, target sparsity + sparsity step, target sparsity + 2*sparsity step].

We empirically find that, for LLaMA2-7B model that contains 32 layers, a discrete sparsity set of

Search	L1-7B	L1-13B	L2-7B	L2-13B	L3-8B	L3-8B-it	M-7B	M-7B-it
Metric	1h10m28s	2h13m6s	1h6m14s	2h11m55s	1h30m47s	1h31m51s	1h14m22s	1h15m54s
Ratio	1h13m44s	2h19m28s	1h9m34s	2h22m45s	1h31m59s	1h32m51s	1h17m8s	1h18m12s

Table 11: Cost of searching for optimal pruning metric and layerwise sparsity ratios on LLaMA-1/2/3 and Mistral models.

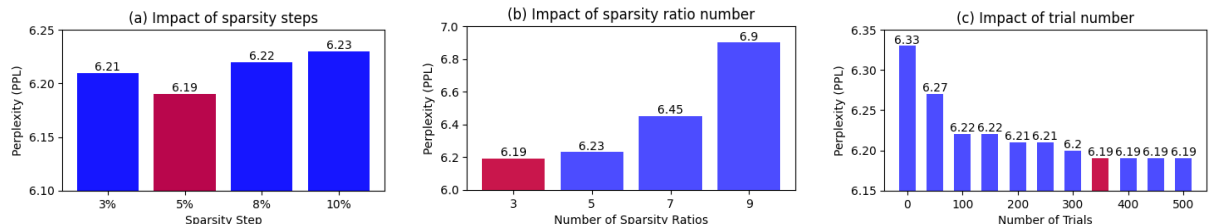


Figure 5: Sensitivity evaluation on sparsity step, number of sparsity ratios, and the number of trials in layerwise sparsity ratio search.

coefficient	Equation	coefficient	Equation
no coe	$\alpha = \beta = 1$	F norm	$\alpha = \beta = 1/\sqrt{\sum_{i=1}^m \sum_{j=1}^n A_{ij}^2}$
to sum	$\alpha = \beta = 1/\sum_{i=1}^m \sum_{j=1}^n A_{ij}$	to mean	$\alpha = \beta = mn/\sum_{i=1}^m \sum_{j=1}^n A_{ij}$
row sum	$\alpha = \beta = 1/\sum_{j=1}^n A_{ij}$	column sum	$\alpha = \beta = 1/\sum_{i=1}^m A_{ij}$
relative sum	$\alpha = \beta = \text{row sum } (A_{ij}) + \text{column sum } (A_{ij})$		

Table 12: Detailed calculations for the coefficient sets in meta pruning metric.

3 sparsity ratios is able to search for better results than larger sets of sparsity ratios. This possibly because a larger number of sparsity ratios significantly expands the search space, making it challenging to find the optimal solution within a limited number of search trials.

Number of search trials. In Figure 5(c), we investigate the influence of varying the number of trials on the performance of the NSGA-III search algorithm. The trials evaluated range from an initial count of 0 up to a maximum of 500. The results reveals that the perplexity stabilizes and reaches an optimal value at the point where the number of search trials is set to 350. Based on this empirical evidence, we select this specific number of trials for the NSGA-III algorithm in our experiments discussed in the main paper.

A.6 Optimal Pruning Metric and Layerwise Sparsity Ratios

Our meta pruning metric adjusts the relationship between weight and activation magnitudes by applying specific coefficients and operations to both weight and activation magnitudes. The operation sets include (1) no op, which leaves the matrix unchanged, (2) sqrt, which computes the square root of each matrix element, and (3) square, which raises each element to the power of two. The coefficient sets include (1) no coe, which leaves the scaling of the matrix elements unchanged, (2) F norm, using the reciprocal of the Frobenius norm of the matrix, (3) to sum, and (4) to mean, setting the coefficients as the reciprocal of the total sum and the average of the matrix elements, respectively. (5) row sum and (6) column sum, using the reciprocal of the sums of specific rows or columns, respectively. Finally, (7) relative sum calculates coefficients as the sum of the row sums and column sums for each matrix element. The detailed calculation equations are illustrated in Table 12, using matrix $A = A_{ij}$ with m rows and n columns as input for demonstration.

The detailed calculations for the coefficient sets utilized in our pruning metric are comprehensively illustrated in Table 12. For these calculations, we use a matrix $A = A_{ij}$ that consists of m rows and n columns as input demonstration.

Optimal pruning metrics. In Table 13, we present the optimal coefficients and operations for pruning metrics using samples from the C4 dataset as calibration data. Table 14 displays the optimal coefficients and operations for pruning metrics using samples from the GSM8K dataset as calibration data. Compared to the results based on the C4 dataset, the metrics derived from the GSM8K dataset show a greater divergence from RIA metric (Zhang et al.). Notably, most of these metrics do not incorporate the relative sum as a weight coefficient.

Optimal layerwise pruning ratio. In Figure 6, we report the optimal layerwise sparsity ratios for LLaMA-1/2/3 and Mistral models. The results generally indicate that the upper layers contain more redundant parameters compared to the lower layers, as higher sparsity ratios are more common in the top layers, while lower sparsity ratios are more frequent in the lower layers.

A.7 Relationship between Transformed Wights and Activations

In our analysis of the optimal searched pruning metrics, We find that the differences between transformed weights and transformed activations may affect the effectiveness of different pruning metrics. Specifically, we analyze each pruning metric, such as Wanda, RIA, and OptiShear, by decomposing them into two distinct components: the transformed weights and the transformed activations, each defined by specific coefficients or operations. As the SparseGPT metric combines weights and the Hessian matrix, and the Wanda metric serves as a simpler approximation of the SparseGPT metric. Due to this relationship, we omit the weight and activation analysis for SparseGPT.

Metric	LLaMA-1		LLaMA-2		LLaMA-3		Mistral	
	7B	13B	7B	13B	8B	8B-Inst	7B	7B-Inst
α	relative sum	relative sum	relative sum	relative sum	relative sum	no coe	relative sum	F norm
β	to mean	to mean	to mean	no coe	F norm	F norm	to mean	to mean
τ_1	no op	square	no op	square	no op	no op	square	sqrt
τ_2	sqrt	no op	sqrt	sqrt	no op	no op	no op	sqrt

Table 13: Optimal coefficients and operations for pruning metrics on C4 calibration data.

Metric	LLaMA-1		LLaMA-2		LLaMA-3		Mistral	
	7B	13B	7B	13B	8B	8B-Inst	7B	7B-Inst
α	row sum	to mean	F norm	column sum	to mean	relative sum	row sum	relative sum
β	relative sum	F norm	to sum	relative sum	to sum	no coe	no coe	to mean
τ_1	no op	no op	no op	square	square	no op	square	square
τ_2	sqrt	sqrt	sqrt	sqrt	sqrt	no op	no op	no op

Table 14: Optimal coefficients and operations for pruning metrics on GSM8K calibration data.

We measure the difference between transformed weights and activations as the layer-wise absolute difference, which is calculated by summing the average absolute differences across all linear sub-modules in each layer. We report the average layer-wise differences between the operated weights and the operated activations across the Wanda, RIA, and OptiShear pruning metrics in Table 15, with detailed layer-wise difference curves available in Figures 7, 8, 9, 10.

Table 15 shows that the RIA pruning metric reduces the absolute difference compared to Wanda, while the OptiShear searched metric further minimizes this difference, bringing it close to zero. The weighted transformation operation in the OptiShear pruning metric effectively scales both weights and activations into a similar numerical range, facilitating a balanced evaluation of each weight relative to its corresponding activation.

Coupled with the performance results of each pruning metric presented in Table 2, the difference analysis in Table 15 suggests that pruning metrics with smaller absolute differences between transformed weights and activations are more likely to achieve effective pruning. Thus, the performance of Wanda and other methods may be influenced by how well they account for these differences regarding different models with different weight magnitudes and distributions.

A.8 Task-wise Results on LM Harness

For LM-harness results, the 7 evaluated zero-shot tasks are: BoolQ (Clark et al., 2019), RTE (Wang et al., 2018), HellaSwag (Zellers et al., 2019),

WinoGrande (Sakaguchi et al., 2021), ARC Easy and Challenge (Clark et al., 2018), and OpenbookQA (Mihaylov et al., 2018). For reproducibility, we used v0.4.0 release. All tasks were evaluated on task version 0 except for BoolQ on task version 1. We show the task-wise performance of mean zero-shot accuracies of pruned LLaMA-1/2/3 and Mistral models in Tables 16, 17, 18, 19, 20, 21, 22, 23.

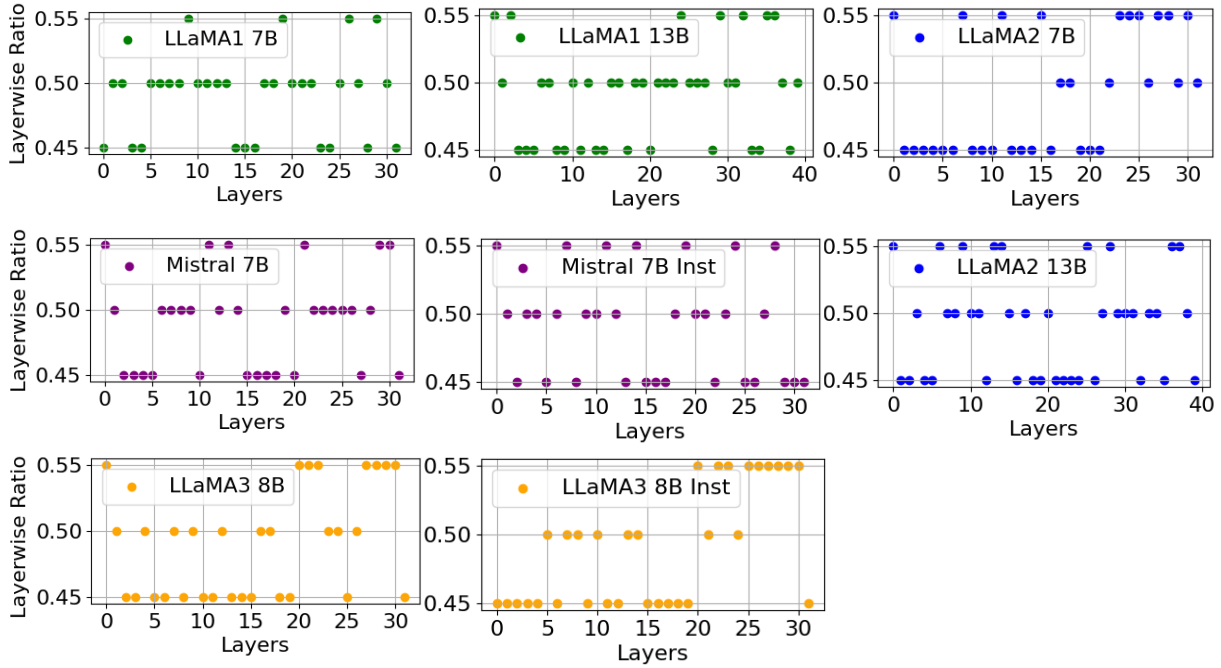


Figure 6: Searched layerwise sparsity ratios for LLaMA-1/2/3 and Mistral models.

Method	LLaMA-2 7B	LLaMA-2 13B	LLaMA-3 8B	Mistral 7B
Wanda	82.66	78.30	79.31	392.13
RIA	22.34	21.91	21.15	44.77
OptiShear	1.09	0.0001	0.1263	0.0304

Table 15: Average absolute difference between operated weights and operated activations for Wanda, RIA and OptiShear on C4 Calibration Data.

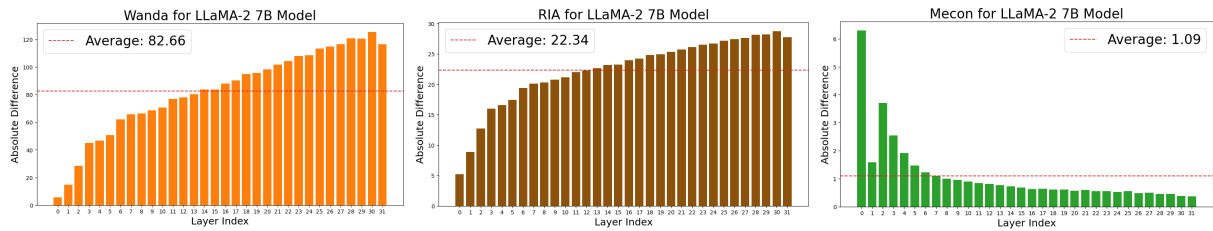


Figure 7: Layerwise absolute distance between transformed weights and transformed activations for Wanda, RIA, and OptiShear metrics on LLaMA-2 7B models.

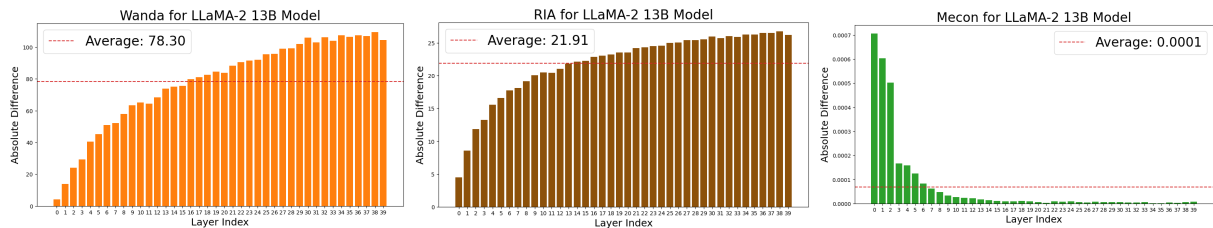


Figure 8: Layerwise absolute distance between transformed weights and transformed activations for Wanda, RIA, and OptiShear metrics on LLaMA-2 13B models.

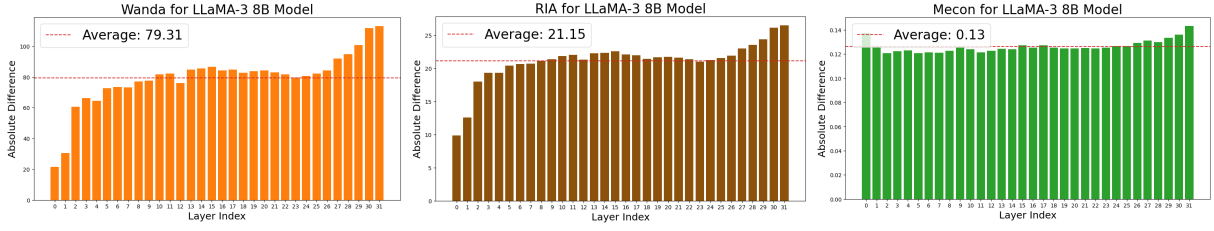


Figure 9: Layerwise absolute distance between transformed weights and transformed activations for Wanda, RIA, and OptiShear metrics on LLaMA-3 8B models.

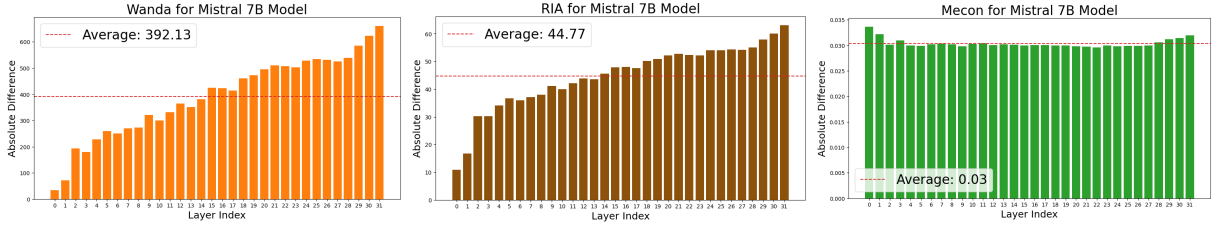


Figure 10: Layerwise absolute distance between transformed weights and transformed activations for Wanda, RIA, and OptiShear metrics on Mistral 7B models.

Method	BoolQ	RTE	HellaSwag	WinoGrande	ARC-e	ARC-c	OBQA	Average
Dense	75.06	66.23	56.93	69.54	74.82	41.02	34.30	59.70
Magnitude	55.10	54.51	45.49	59.10	58.65	32.97	22.40	46.89
SparseGPT	72.03	54.15	51.43	67.87	71.39	37.54	29.60	54.86
Wanda	71.04	54.51	51.93	65.90	69.40	36.95	28.80	54.08
RIA	72.84	57.76	51.93	66.85	70.50	36.43	29.40	55.10
Pruner-Zero	70.28	56.68	47.27	64.96	66.92	33.25	26.80	52.31
Our Metric	72.87	57.40	51.91	67.25	70.33	36.35	29.60	55.10
GSM8K Metric	71.04	58.48	52.39	67.17	69.91	37.46	30.20	55.24
LLaMA2 Metric	70.73	57.63	53.24	67.01	70.24	37.97	30.20	55.15

Table 16: Accuracies (%) of LLaMA-1 7B model for 7 zero-shot tasks with unstructured 50% sparsity.

Method	BoolQ	RTE	HellaSwag	WinoGrande	ARC-e	ARC-c	OBQA	Average
Dense	78.03	70.51	59.63	72.89	77.28	46.55	33.20	62.58
Magnitude	55.19	52.23	43.65	63.36	57.82	32.53	26.60	47.34
SparseGPT	76.89	60.95	54.99	71.46	72.15	42.17	31.20	58.54
Wanda	75.73	62.48	55.70	71.68	72.91	43.45	32.20	59.18
RIA	76.44	62.34	56.13	72.73	72.42	43.87	32.20	59.45
Pruner-Zero	73.91	62.36	52.65	69.41	70.83	41.62	28.80	57.08
Our Metric	76.67	62.45	56.11	73.63	73.25	43.62	32.40	59.73
GSM8K Metric	76.62	62.89	55.48	72.79	72.58	43.78	32.00	59.45
LLaMA2 Metric	76.51	62.32	56.43	71.82	73.39	43.84	32.40	59.53

Table 17: Accuracies (%) of LLaMA-1 13B model for 7 zero-shot tasks with unstructured 50% sparsity.

Method	BoolQ	RTE	HellaSwag	WinoGrande	ARC-e	ARC-c	OBQA	Average
Dense	77.74	62.82	57.14	69.14	76.35	43.43	31.40	59.72
Magnitude	62.57	52.35	52.99	65.35	67.97	37.20	28.40	52.40
SparseGPT	75.78	57.75	52.90	69.14	71.34	37.97	26.60	55.90
Wanda	75.35	53.43	52.63	67.25	72.35	39.42	30.80	55.89
RIA	75.66	53.79	52.25	67.25	72.05	37.71	31.00	55.67
Pruner-Zero	73.48	53.29	49.18	65.83	69.92	38.36	26.60	53.81
Our Metric	74.62	62.82	57.14	68.03	71.00	38.91	29.80	57.47
GSM8K Metric	75.11	53.79	53.55	67.25	72.31	39.93	30.40	56.05
LLaMA2 Metric	75.11	53.79	53.55	67.25	72.31	39.93	30.40	56.05

Table 18: Accuracies (%) of LLaMA-2 7B model for 7 zero-shot tasks with unstructured 50% sparsity.

Method	BoolQ	RTE	HellaSwag	WinoGrande	ARC-e	ARC-c	OBQA	Average
Dense	80.52	65.34	60.33	71.95	79.38	48.47	35.20	63.03
Magnitude	57.62	55.87	54.53	65.85	70.47	38.13	27.80	52.90
SparseGPT	81.42	65.26	55.83	72.64	74.91	42.23	32.60	60.70
Wanda	81.86	64.08	56.92	71.37	76.12	43.81	32.00	60.88
RIA	81.93	64.02	57.73	71.89	76.24	43.46	32.00	61.03
Pruner-Zero	77.86	61.22	56.89	67.90	74.16	39.81	29.40	58.18
Our Metric	80.97	66.17	59.68	72.35	76.29	43.68	30.80	61.42
GSM8K Metric	81.56	64.06	58.41	72.23	76.98	43.73	32.00	61.28
LLaMA2 Metric	80.25	66.14	59.73	71.57	77.36	43.85	32.00	61.56

Table 19: Accuracies (%) of LLaMA-2 13B model for 7 zero-shot tasks with unstructured 50% sparsity.

Method	BoolQ	RTE	HellaSwag	WinoGrande	ARC-e	ARC-c	OBQA	Average
Dense	81.44	69.68	60.17	72.85	80.09	50.43	34.80	64.21
Magnitude	49.14	53.43	38.55	55.09	60.69	32.42	24.80	44.87
SparseGPT	74.80	54.15	49.90	68.35	67.05	36.43	26.40	53.87
Wanda	73.43	52.71	41.80	63.22	64.86	29.78	21.80	49.66
RIA	75.20	53.12	43.00	64.56	65.87	30.55	23.00	50.76
Pruner-Zero	72.32	54.51	45.78	65.19	70.58	35.41	23.60	52.48
Our Metric	79.54	53.07	43.24	70.24	72.05	41.13	29.20	55.50
GSM8K Metric	73.88	63.90	49.68	68.90	70.37	37.80	24.60	55.59
LLaMA3 Metric	73.88	63.90	49.68	68.90	70.37	37.80	24.60	55.59

Table 20: Accuracies (%) of LLaMA-3 8B model for 7 zero-shot tasks with unstructured 50% sparsity.

Method	BoolQ	RTE	HellaSwag	WinoGrande	ARC-e	ARC-c	OBQA	Average
Dense	83.06	67.51	57.68	71.98	81.61	52.99	34.20	64.15
Magnitude	68.84	60.65	36.31	53.75	49.83	26.19	21.80	45.31
SparseGPT	77.00	60.65	49.61	66.46	70.92	40.19	26.40	55.89
Wanda	76.57	54.51	41.18	63.61	67.63	33.70	22.20	51.34
RIA	78.17	54.51	42.29	64.25	68.35	34.13	22.80	50.64
Pruner-Zero	76.88	54.51	45.32	65.67	69.44	36.95	25.00	55.60
Our Metric	81.56	54.15	42.32	68.11	74.28	41.55	29.60	55.94
GSM8K Metric	78.17	54.51	42.29	64.25	68.35	34.13	22.80	50.64
LLaMA3 Metric	76.82	62.45	48.18	66.30	71.34	39.59	26.80	55.93

Table 21: Accuracies (%) of Instruction-tuned LLaMA-3 8B model for 7 zero-shot tasks with unstructured 50% sparsity.

Method	BoolQ	RTE	HellaSwag	WinoGrande	ARC-e	ARC-c	OBQA	Average
Dense	81.44	69.68	60.17	72.85	80.09	50.43	34.80	64.21
Magnitude	75.87	55.60	56.74	68.35	74.20	42.15	27.80	57.24
SparseGPT	76.73	61.01	54.52	67.72	74.24	41.64	26.60	57.49
Wanda	76.12	55.60	48.95	65.59	72.69	37.46	23.00	54.20
RIA	76.48	56.68	49.05	66.30	72.47	37.12	22.60	54.39
Pruner-Zero	77.46	60.65	50.25	68.90	71.84	37.46	22.40	55.57
Our Metric	82.35	56.68	55.77	70.88	76.18	45.22	28.22	59.33
GSM8K Metric	81.53	55.60	54.43	69.38	74.16	42.15	26.40	57.66
LLaMA3 Metric	80.52	56.32	55.94	69.53	75.00	42.41	28.40	58.30

Table 22: Accuracies (%) of Mistral 7B model for 7 zero-shot tasks with unstructured 50% sparsity.

Method	BoolQ	RTE	HellaSwag	WinoGrande	ARC-e	ARC-c	OBQA	Average
Dense	83.06	67.51	57.68	71.98	81.61	52.99	34.20	64.15
Magnitude	79.09	65.06	59.31	67.43	77.96	49.77	31.80	62.34
SparseGPT	81.56	72.92	58.77	70.01	76.85	48.72	28.40	62.46
Wanda	83.73	66.79	55.68	67.48	77.06	48.12	28.40	61.04
RIA	83.88	66.79	55.61	67.32	77.78	47.95	27.60	60.48
Pruner-Zero	83.18	68.95	56.17	68.27	76.43	47.44	29.40	61.41
Our Metric	84.40	66.79	58.75	70.24	80.13	51.45	32.80	63.51
GSM8K Metric	84.59	67.87	58.97	68.90	78.11	51.11	31.80	63.05
LLaMA3 Metric	84.13	66.06	59.87	69.14	78.79	51.37	32.00	63.05

Table 23: Accuracies (%) of Instruction-tuned Mistral 7B model for 7 zero-shot tasks with unstructured 50% sparsity.